The balance between gasdermin D and STING signaling shapes the severity of schistosome immunopathology

Parisa Kalantari[a,b,1], Ilana Shecter[a], Jacob Hopkins[a], Andrea Pilotta Gois[a], Yoelkys Morales[a], Bijan F. Harandi[a] (ID), Shruti Sharma[a] (ID), and Miguel J. Stadecker[a] (ID)

There is significant disease heterogeneity among mouse strains infected with the helminth *Schistosoma mansoni*. Here, we uncover a unique balance in two critical innate pathways governing the severity of disease. In the low-pathology setting, parasite egg-stimulated dendritic cells (DCs) induce robust interferon (IFN)β production, which is dependent on the cyclic GMP-AMP synthase (cGAS)/stimulator of interferon genes (STING) cytosolic DNA sensing pathway and results in a Th2 response with suppression of proinflammatory cytokine production and Th17 cell activation. IFNβ induces signal transducer and activator of transcription (STAT)1, which suppresses CD209a, a C-type lectin receptor associated with severe disease. In contrast, in the high-pathology setting, enhanced DC expression of the pore-forming protein gasdermin D (Gsdmd) results in reduced expression of cGAS/STING, impaired IFNβ, and enhanced pyroptosis. Our findings demonstrate that cGAS/STING signaling represents a unique mechanism inducing protective type I IFN, which is counteracted by Gsdmd.

STING | type I IFN | gasdermin D | CD209a | STAT1

Schistosomes are trematode helminths that infect more than 250 million people, of which 120 million suffer from clinical morbidity (1). Infection with the species *Schistosoma mansoni* (*S. mansoni*) targets the liver and intestines, where trapped parasite eggs trigger a CD4 T helper (Th) cell–mediated granulomatous inflammation and fibrosis. Most schistosome-infected individuals develop a relatively mild form of the disease; however, in 5 to 10% of the patients, the disease is severe and life threatening (2). Despite the large disease burden, schistosomiasis remains a neglected disease with limited insights into disease pathogenesis and immunopathological heterogeneity.

Intriguingly, a disease dichotomy is observed in the murine model of schistosomiasis, where C57BL/6 (BL/6) mice develop milder pathology amidst a protective antiinflammatory Th2-dominated cytokine environment (2), whereas CBA mice develop severe hepatic egg-induced immunopathology, largely mediated by proinflammatory Th17 cells (3–5). Our previous studies have highlighted how disparate T cell responses in the two backgrounds rely on differences in key innate immune components such as antigen-presenting cells (APCs). Indeed, differences in the expression of key innate immune factors in dendritic cells (DCs) are central to shaping immunopathogenicity during schistosomiasis (6–8). The establishment of a net antiinflammatory milieu is therefore a key requisite to avert severe disease (9–12). To date, the signaling pathways resulting in dissimilar levels of pathology remain incompletely understood and are key to appreciating how genetic differences result in dissimilar disease severity.

To ascertain key immune genes that may be the basis of disease heterogeneity, we performed a gene array and identified C-type lectin receptor (CLR), dendritic cell-specific ICAM-3-grabbing nonintegrin (DC-SIGN, CD209), as a key determinant of schistosome immunopathology (6, 13). DC-SIGN/CD209 plays a crucial role in the recognition of pathogens such as HIV, Ebola virus, mycobacteria, opportunistic fungi, and schistosomes (14–17). CD209a (SIGNR5) is the closest murine homolog to human DC-SIGN and its expression is strikingly elevated in DCs from high-pathology CBA mice vs. low-pathology BL/6 mice. Our previous studies highlight a decisive role for CD209a in shaping subsequent T cell skewing and immunopathology, as schistosome-infected CBA CD209a$^{-/-}$ mice display markedly reduced Th17 cell responses and hepatic granulomatous lesions (6). Mechanistically, CD209a synergizes with Dectin-2 and Mincle to facilitate IL-1β and IL-23 production by egg-stimulated DCs necessary for pathogenic Th17 cell activation (6).

Schistosome eggs have been reported to stimulate DCs to produce type I IFN (IFN-I), a large family of cytokines including 14 IFNα in mice (13 in humans) and IFNβ. IFN-I subsequently induces a proresolving Th2 response by signaling through the heterodimeric IFN-I receptor (IFNAR) (18, 19). Yet, multiple aspects of the IFN-I relationship to

Significance

Schistosomes cause widespread disease in vertebrates and are responsible for over 200 million human infections worldwide. Most schistosome-infected patients develop a mild form of the disease; however, for 5 to 10% of the patients, the disease is severe and life threatening. To date, the molecular mechanisms resulting in such widely dissimilar pathology remain poorly understood. We now report that in low-pathology setting, cyclic GMP-AMP synthase/stimulator of interferon genes (cGAS/STING)-dependent type I interferon (IFN-I) down-regulates dendritic cell (DC) expression of CD209a, with consequent dampening of IL-1β, IL-23, and Th17 cell activation, as well as increased Th2 cytokines, resulting in the amelioration of immunopathology. Additionally, Gsdmd, which is highly expressed in high-pathology setting, reduces egg-mediated IFN-I responses via induction of pore formation and enhanced pyroptosis.

schistosomiasis remain unknown, including which pathways regulate the induction of IFN-I during disease and how IFNAR signaling impacts disease severity.

Innate detection of aberrantly localized DNA is a predominant trigger for IFN-I production and a vital component of host defense. Cytosolic DNA is sensed by cyclic guanosine monophosphate adenosine monophosphate synthase (cGAS), which generates a small, heterodimeric, endogenous secondary messenger cyclic GMP-AMP (cGAMP) from cytosolic pools of Adenosine triphosphate (ATP) and Guanosine-5'-triphosphate (GTP). cGAMP in turn binds to the C-terminal domain of the endoplasmic reticulum (ER)-resident signaling adaptor, stimulator of IFN genes (STING) (gene: *Tmem173*) (20, 21), leading to the transcription of IFN-I (reviewed in refs. 21 and 22). Recent studies have revealed an outsized role for innate pathways that sense cytosolically localized microbial DNA in host defense against various pathogens such as *Plasmodium* (23), HIV (24), and *Mycobacterium tuberculosis* (25). Both IFN-I and cGAS/STING pathways play key roles in controlling disease pathogenesis by either limiting or enhancing inflammation, depending on the disease setting (26–29). Surprisingly, a role for the cGAS/STING pathway in helminth infections remains entirely unexplored.

In order to explore the cellular and molecular origin of IFN-I during schistosomiasis and pinpointing its role in disease severity, we investigated the contribution of cGAS/STING during schistosomiasis. Here, we report that stimulation of low-pathology BL/6 DCs with live schistosome eggs induces robust IFNβ production in a cGAS/STING/IFNAR-dependent manner. The absence of cGAS/STING signaling resulted in heightened expression of proinflammatory IL-1β and IL-23 responses and mobilization of Th17 cells, simulating a high-pathology response. Consistent with these results, BL/6 mice lacking STING exhibited significantly enhanced hepatic granulomatous inflammation associated with increased Th17 and diminished Th2 cell responses. Mechanistically, we show that cGAS/STING-mediated Th17 suppression is a direct result of the downregulation of the high-pathology driving CLR, CD209a. Gsdmd was highly expressed in CBA DCs, leading to reduced expression of cGAS/STING, diminished IFNβ, and heightened pyroptosis, when stimulated with eggs. These findings unravel unique mechanisms by which cGAS/STING-dependent signals restrain immunopathology. They also provide insights into an unrecognized role of Gsdmd in modulating the protective IFN-I pathway in schistosomiasis.

Results

Egg-Induced DC IFNβ Production Depends on cGAS/STING/ IFNAR, Correlates with Reduced Proinflammatory Cytokines, and Skews Toward an Enhanced IL-4 Response. Previous gene profiling from our laboratory revealed an IFN-I signature in bone marrow derived dendritic cells (BMDCs) from low-pathology BL/6 mice in the form of elevated interferon-stimulated gene (ISG) expression such as Ccl5, Stat4, Slamf7, and Ccl22, whereas proinflammatory gene expression was elevated in BMDCs from high-pathology CBA mice (7). To investigate whether the low pathology is linked to a protective IFN-I response, we measured IFNβ in livers from uninfected and infected CBA and BL/6 mice. Indeed, there was a marked increase of IFNβ in BL/6 livers and spleens, suggesting a role for this cytokine in controlling disease severity (Fig. 1*A*).

IFN-I production can result from the activation of four distinct pathways: cGAS/STING as well as retinoic acid-inducible gene I (RIG-I)/mitochondrial antiviral-signaling protein (MAVS) are cytosolic pathogen recognition receptors (PRRs) that recognize

DNA and RNA, respectively (30), whereas myeloid differentiation primary response 88 (MyD88) (31) and TIR-domain-containing adapter-inducing interferon β (TRIF) (32) are adaptor proteins triggered by Toll-like receptors. We investigated the role of these pathways in IFN-I production in the setting of the schistosome infection using egg-stimulated BMDCs from BL/6 and CBA mice. STING expression was strikingly higher in BL/6 BMDCs, while no differences were observed in the expression of MAVS and MyD88 (Fig. 1 *B*, *Left*). Moreover, there was no significant difference in IFNβ production between egg-stimulated *Trif*$^{-/-}$ BMDCs and BL/6 wild-type (WT) controls (Fig. 1 *B*, *Right*), all suggesting that cytosolic cGAS/STING-dependent DNA sensing is a critical trigger of IFN-I production in BL/6 mice.

Stimulation with schistosome eggs (Fig. 1 *C*, *Left*) as well as transfection with *S. mansoni* genomic DNA (*Sm* gDNA) (Fig. 1 *C*, *Right*) induced IFNβ production in BL/6 but not in *STING*$^{-/-}$ BMDCs in vitro, with poly (dAdT) serving as a positive control. Similarly, BMDCs lacking cGAS, whether stimulated with eggs or *Sm* gDNA (Fig. 1*D*) or IFNAR1 (Fig. 1*E*), produced significantly less IFNβ, suggesting that, together with STING, cGAS and IFNAR1 are members of the same signaling pathway activated by gDNA. Consistent with these results, cGAMP levels were significantly diminished in egg-stimulated *cGAS*$^{-/-}$ BMDCs (*SI Appendix*, Fig. S1A). We next assessed how STING-, cGAS-, and IFNAR1-dependent signaling affects cytokines regulating inflammation in schistosomiasis. Egg stimulation of *STING*$^{-/-}$ BMDCs resulted in a significant increase in IL-1β (Fig. 1 *F*, *Left*) and IL-23 (Fig. 1 *I*, *Left*), or in enhanced IL-17 production by BMDC-T cell cocultures (Fig.1 *L*, *Left*). IL-1β (*SI Appendix*, Fig. S1 *B*, *Left*) and IL-23 (*SI Appendix*, Fig. S1 *B*, *Right*) were also increased in *cGAS*$^{-/-}$ BMDCs transfected with *Sm* gDNA. The absence of cGAS and IFNAR1 similarly resulted in increases in IL-1β (Fig. 1 *G* and *H*), IL-23 (Fig. 1 *J* and *K*), and IL-17 (Fig. 1 *M* and *N*). In contrast, the Th2 cytokine IL-4 produced by *STING*$^{-/-}$ (Fig. 1O), *cGAS*$^{-/-}$ (Fig. 1P), and *IFNAR1*$^{-/-}$ (Fig. 1Q) BMDC-T cell cocultures was significantly lower than that in WT controls. These results build upon a recent report suggesting a role for IFN-I in initiating DC-dependent Th2 responses to schistosome eggs (18). Additionally, we showed that IL-4 was produced by CD4 T cells and not BMDCs (*SI Appendix*, Fig. S1C). Lastly, the loss of STING (*SI Appendix*, Fig. S1 *D*, *Left*), cGAS (*SI Appendix*, Fig. S1 *D*, *Center*), or IFNAR1 (*SI Appendix*, Fig. S1 *D*, *Right*) had no effect on TNFα production, suggesting that alternate pathways regulate this cytokine.

To further define the role of STING in suppressing proinflammatory cytokine responses, we transduced *STING*$^{-/-}$ BMDCs with STING retroviruses. This approach resulted in a full restitution of STING expression (*SI Appendix*, Fig. S1E), as well as STING-mediated suppression of IL-1β (Fig. 1 *F*, *Center*) and IL-23 (Fig. 1 *I*, *Center*) production. To further test whether the STING-dependent suppression of proinflammatory cytokines operated via IFN-I, we added IFNβ to *STING*$^{-/-}$ BMDCs. The exogenous IFNβ induced significant inhibition of IL-1β (Fig. 1 *F*, *Right*) and IL-23 (Fig. 1 *I*, *Right*) production by egg-stimulated *STING*$^{-/-}$ BMDCs, and of IL-17 (Fig. 1 *L*, *Right*) in BMDC-T cell cocultures, but had no effect on TNFα (*SI Appendix*, Fig. S1F). Lastly, to verify the inhibitory effect of IFN-I in the natural setting of low IFN-I (Fig. 1*A*), we added IFNβ to egg-stimulated CBA BMDCs. This resulted in a significant inhibition of IL-1β (*SI Appendix*, Fig. S1 *G*, *Left*) and IL-23 (*SI Appendix*, Fig. S1 *G*, *Center*), but had no effect on TNFα (*SI Appendix*, Fig. S1 *G*, *Right*). Taken together, these results suggest that cGAS/STING/ IFNAR1 pathway-dependent IFN-I production suppresses proinflammatory Th1 and Th17 responses while promoting Th2 polarization during schistosome infection.
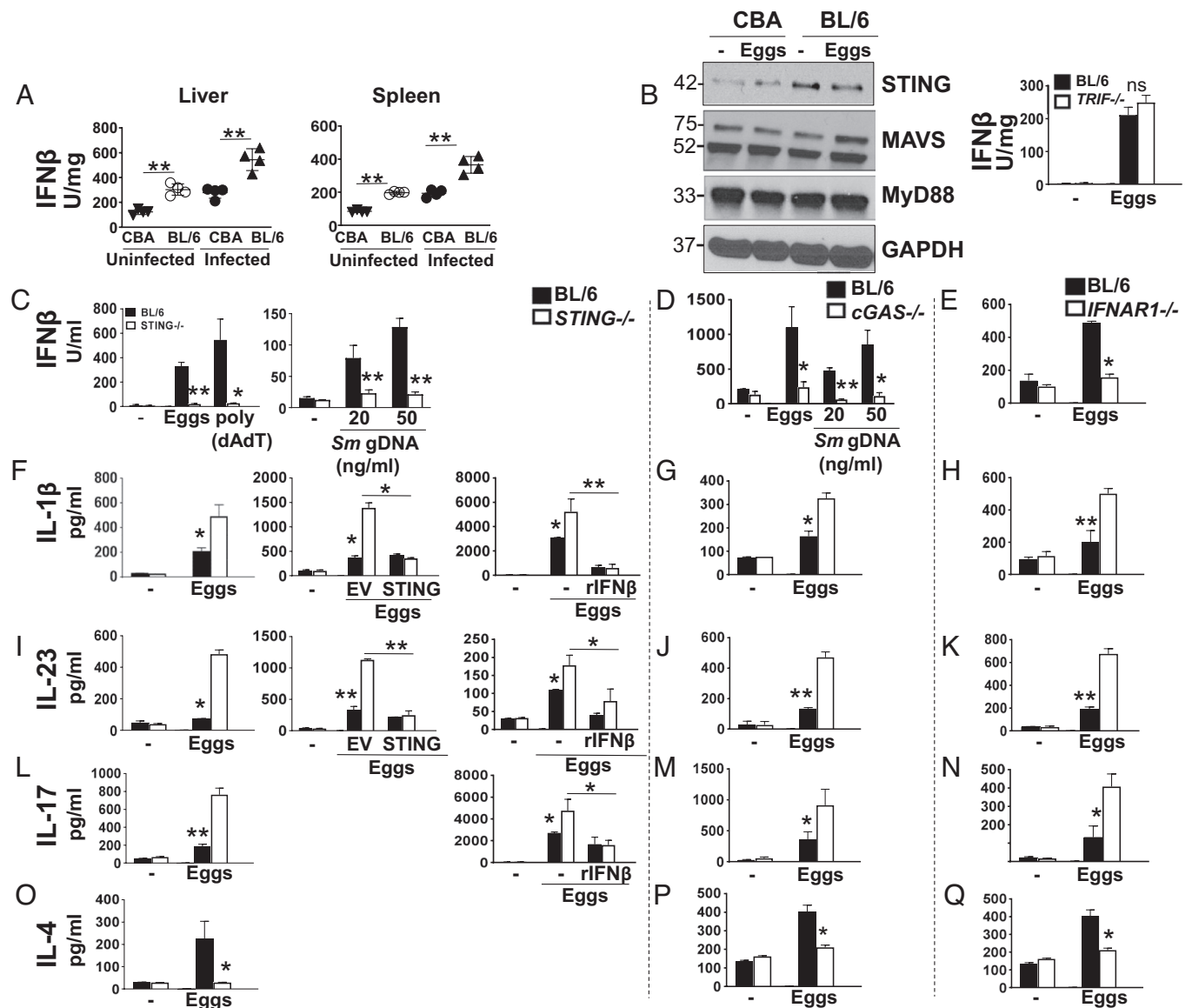
Fig. 1. IFNβ production is diminished while proinflammatory cytokine production is enhanced in the absence of STING, cGAS, and IFNAR1. (*A*) Liver and spleen from uninfected and infected CBA and BL/6 mice were homogenized, and IFNβ levels were assessed by ELISA. (*B*) Immunoblot analysis of 2×10^6 CBA and BL/6 BMDCs plated in six-well plates and stimulated with 1,000 live eggs per well for 24 h. Cell lysates were used for western blot analysis using Abs against STING, MAVS, MyD88, and GAPDH (*Left*). Given the lack of TRIF western blot Abs, TRIF's impact on IFNβ production was assessed by culturing BL/6 and *Trif*$^{-/-}$ BMDCs with 100 live eggs and measuring IFNβ in 24 h supernatants by ELISA (*Right*). BL/6 and STING$^{-/-}$ BMDCs were cultured with 100 live eggs, and cytokines IFNβ (*C, Left*), IL-1β (*F, Left*), IL-23 (*I, Left*), IL-17 (*L, Left*), and IL-4 (*O*) in the supernatants were measured by ELISA. In *C, Left*, BMDCs were also transfected with 1.5 mg/mL poly (dAdT) and in *C, Right*, with the indicated amounts of *Sm* gDNA using Lipofectamine 2000. In *F, Center*, and *I, Center*, BMDCs were transduced with empty vector (EV) or STING before egg stimulation, and in *F, Right*, *I, Right*, and *L, Right*, they were pretreated with rIFNβ for 1 h followed by egg stimulation. BL/6 and cGAS$^{-/-}$ BMDCs were cultured with 100 live eggs, and cytokines IFNβ (*D*), IL-1β (*G*), IL-23 (*J*), IL-17 (*M*), and IL-4 (*P*) in the supernatants were measured by ELISA. In (*D*) BMDCs were also transfected with indicated amounts of *Sm* gDNA using Lipofectamine 2000. BL/6 and IFNAR1$^{-/-}$ BMDCs were cultured with 100 live eggs, and cytokines IFNβ (*E*), IL-1β (*H*), IL-23 (*K*), IL-17 (*N*), and IL-4 (*Q*) in the supernatants were measured by ELISA. For this and all figures, in order to measure IFNβ, IL-1β, and IL-23, cultures proceeded for 24 h, and for IL-17 and IL-4, cultures also included CD4 T cells and proceeded for 72 h. Bars represent the mean ± SD cytokine levels of three biological replicates from one representative experiment of three with similar results. *$P \leq 0.05$, **$P \leq 0.005$, ns: not significant.

STING Deficiency Results in Marked Increase in Egg-Induced Granulomatous Inflammation. To investigate the role of STING in the development of egg-induced hepatic immunopathology, *STING*$^{-/-}$ and BL/6 mice were infected with *S. mansoni*. After a 7-wk infection, livers, spleens, and mesenteric lymph nodes (MLNs) were all significantly larger (Fig. 2*A*) and heavier (Fig. 2*B*) in *STING*$^{-/-}$ vs. BL/6 controls. The livers of *STING*$^{-/-}$ mice exhibited a yellowish, granular surface denoting granulomatous lesions, which were more prominent than those seen in BL/6 controls (Fig. 2*A*). Upon histological analysis, the granulomas were composed of mono- and polynuclear inflammatory cells surrounding central eggs. In *STING*$^{-/-}$ mice, they were significantly larger and had

less defined borders with more cells spilling into the surrounding hepatic parenchyma (Fig. 2*C*). Morphometric analysis of single-egg granulomas confirmed that the average granuloma size in *STING*$^{-/-}$ mice was significantly larger than that in BL/6 mice (Fig. 2*D*); however, the number of eggs present in the livers did not significantly differ between the mouse groups, indicating that the parasite load did not correlate with the extent of inflicted pathology (Fig. 2*E*).

STING Deficiency Leads to Enhanced Th17/Th1 and Diminished Th2 Cytokine Responses In Vivo and Ex Vivo. To further assess the impact of STING during in vivo infection, cytokine
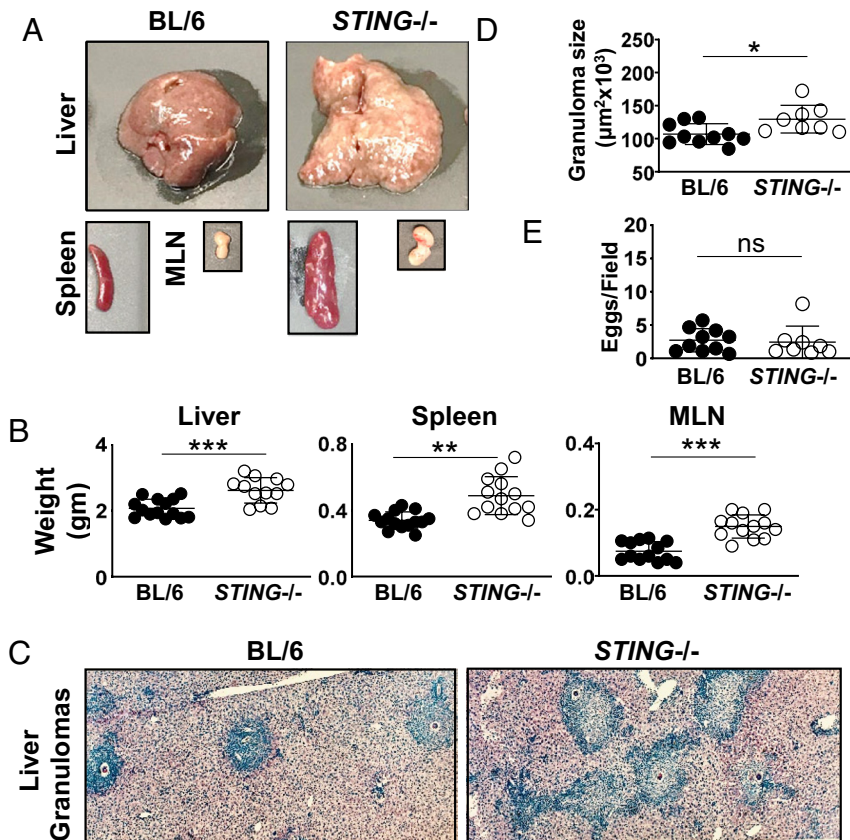
Fig. 2. $STING^{-/-}$ mice exhibit enhanced egg-induced granulomatous inflammation. (*A*) Representative images of livers, spleens, and MLNs from BL/6 and $STING^{-/-}$ mice infected with *S. mansoni* and killed at 7 wk post infection. (*B*) Weights of livers, spleens, and MLNs from infected BL/6 and $STING^{-/-}$ mice. (*C*) Representative histopathology of liver granuloma of BL/6 and STING$^{-/-}$ mice (magnification, 100×) (*D*) Granuloma size determined by computer-assisted morphometric analysis. Each dot represents average granuloma size of 10 to 20 granulomas in two sections from individual mice. (*E*) Number of eggs per 2.4 mm^2 field assessed on H&E-stained liver sections at 100× magnification. An average of 16 fields per liver section was assessed. Images are representative of three independent experiments. Data in *B*, *D*, and *E* represent pooled results from two or three independent experiments with 3 to 5 mice per group. *$P \leq 0.05$, **$P \leq 0.005$, ***$P \leq 0.0005$, ns: not significant.

responses were measured in liver and spleen homogenates from 7 wk-infected $STING^{-/-}$ and BL/6 mice. In agreement with the in vitro findings, the lack of STING resulted in a marked drop of IFNβ in both organs. There were also significant increases in IL-1β, IL-23, IL-17, and IFNγ, while IL-4, IL-5, and IL-13 were significantly lower (Fig. 3*A*). Ex vivo restimulation of splenic and MLN cells (MLNCs) with live eggs led to a similar shift in cytokine responses in the absence of STING (Fig. 3*B*). However, the loss of STING had no significant effect on liver and spleen TNFα production in vivo (*SI Appendix*, Fig. S2*A*) or following restimulation with eggs of splenic or MLNCs ex vivo (*SI Appendix*, Fig. S2*B*). Taken together, these results suggest that STING restrains proinflammatory cytokines while promoting Th2 cytokines during schistosome infection.

STING Suppresses CD209a Expression and Function via IFN-I Signaling. Stimulation via the CLR CD209a activates pathogenic Th17 cell responses associated with severe egg-induced immunopathology (6). To determine whether STING ameliorates pathology by regulating CD209a, we measured CD209a expression in liver samples and in BMDCs from $STING^{-/-}$ and BL/6 mice. In liver samples obtained from both infected and uninfected mice (Fig. 4*A*), as well as in egg-stimulated or -unstimulated BMDC (Fig. 4*B*), CD209a was higher in the absence of STING. Transducing $STING^{-/-}$ BMDCs with STING retroviruses effectively reduced CD209a to levels observed in BL/6 BMDCs, thus demonstrating the ability of STING to suppress

CD209a (Fig. 4*C*). Importantly, we found increased baseline CD209a expression in uninfected livers and unstimulated BMDCs from $STING^{-/-}$ mice (Fig. 4 *A–C*), suggesting a role for constitutive IFN signaling which has been previously reported to be dependent on the STING pathway (33). STING specifically targeted CD209a as Dectin-2 expression was unaffected by the presence or absence of STING (*SI Appendix*, Fig. S3*A*).

To document the ability of CD209a to promote proinflammatory cytokine production, we effectively silenced CD209a in BL/6 and $STING^{-/-}$ BMDCs using specific lentivirally encoded small hairpin RNAs (shRNAs) (*SI Appendix*, Fig. S3*B*). The CD209a knockdown resulted in a striking reduction of IL-1β (Fig. 4 *D*, *Left*), IL-23 (*SI Appendix*, Fig. S3*C*), and IL-17 (Fig. 4 *D*, *Right*) in BMDCs with no impact on the control vector-enhanced green fluorescent protein (EGFP).

IFNα has been shown to negatively regulate CD209 (DC-SIGN) expression in human monocytes at mRNA and protein levels (34) although the mechanism of this suppression was not examined. To directly address the basis of the STING-regulated CD209a expression, we added rIFNβ to egg-stimulated BL/6 and $STING^{-/-}$ BMDCs. We observed that exogenous IFNβ effectively lowered CD209a in egg-stimulated and -unstimulated $STING^{-/-}$ BMDCs to BL/6 WT levels (Fig. 4*E*), demonstrating that IFNβ can directly regulate CD209a expression. We also evaluated cGAS and IFNAR1 for their ability to modulate CD209a independently, given their impact on BMDC cytokine production (Fig. 1). We found that the absence of either cGAS (Fig. 4*F*) or IFNAR1 (Fig. 4*G*) resulted in a marked
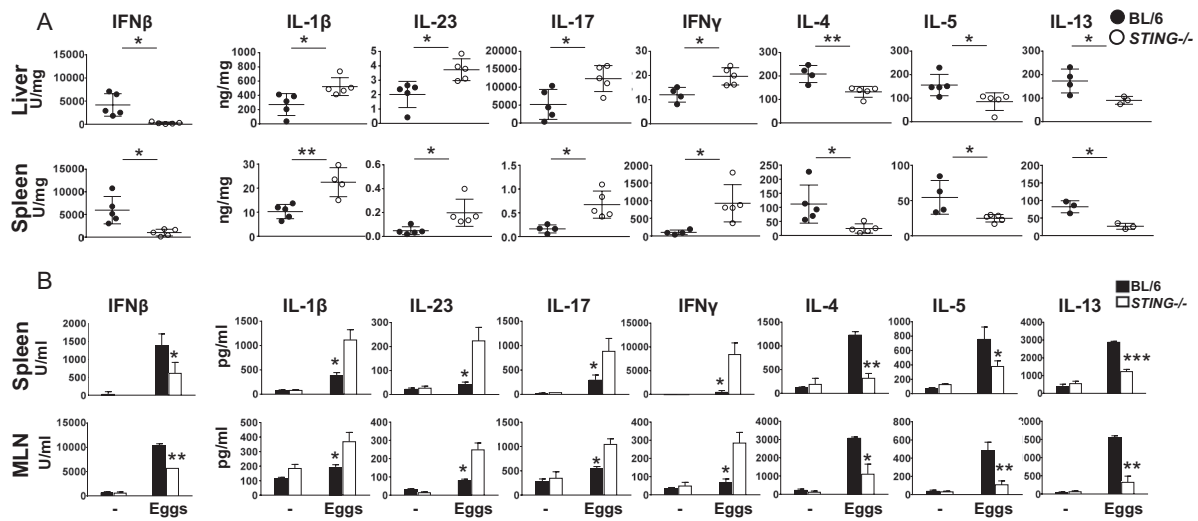
Fig. 3. The absence of STING results in enhanced Th17/Th1 and diminished Th2 cytokine responses in vivo and ex vivo. (*A*) Livers and spleens obtained from infected mice were homogenized and cytokine levels were assessed by ELISA. (*B*) Bulk spleen and MLN from 4 to 5 mice per group were pooled and cultured with live eggs. Cytokines in 72 h supernatants were measured by ELISA. Data in *A* and *B* are representative of one of the three independent experiments with similar results. Each dot (*A*) and bar (*B*) represents mean ± SD cytokine levels of triplicate determinations per mouse. *$P \leq 0.05$, **$P \leq 0.005$.

increase of CD209a in BMDCs, whether stimulated with eggs or not. Taken together, our findings suggest that sequential activation of the cGAS, STING, and IFNAR1 signaling pathway profoundly down-regulates CD209a expression.

IFN-I Suppresses CD209a Promoter Activity via STAT1 Activation. The suppression of CD209a gene transcription by IFN-I signaling prompted us to investigate the involvement of the IFN-I-mediated transcription factor STAT1. IFN-I binds to IFNAR1, which
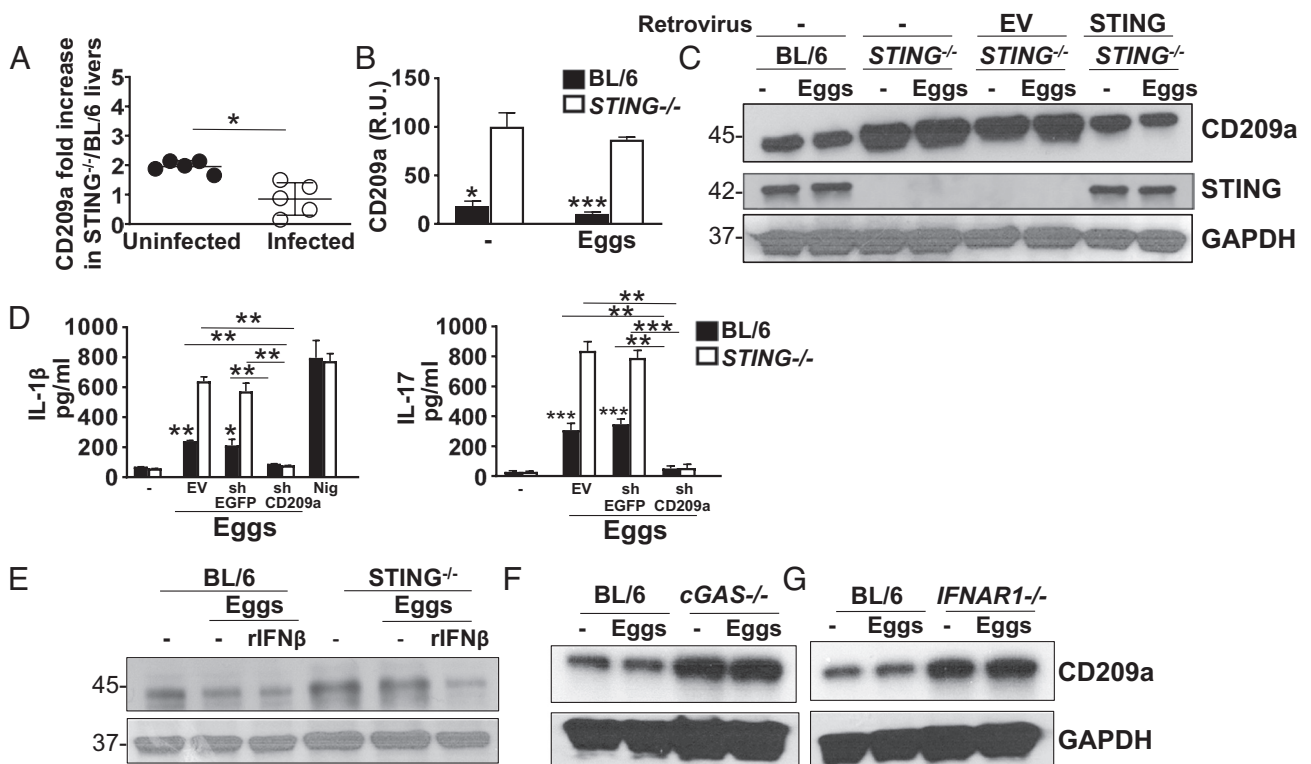

Fig. 4. The loss of STING results in enhanced CD209a expression at mRNA and protein levels. (*A*) Livers obtained from uninfected and infected BL/6 and *STING*$^{-/-}$ mice were homogenized and CD209a levels were assessed by real-time qRT-PCR. Each dot represents mean ± SD CD209a mRNA levels in *STING*$^{-/-}$ liver (normalized to control BL/6 liver) of triplicate determinations per mouse. The CD209a/GAPDH ratio related to uninfected and infected STING$^{-/-}$ liver as well as unstimulated *STING*$^{-/-}$ BMDCs was set to 100. (*B*) 2 × 10^6 BL/6 and STING$^{-/-}$ BMDCs were plated in six-well plates and cultured with or without 1,000 eggs per well for 24 h. CD209a mRNA levels were assessed by real-time qRT-PCR (R.U. = relative units). (*C*) 2 × 10^6 BL/6 and *STING*$^{-/-}$ BMDCs were plated in six-well plates and *STING*$^{-/-}$ BMDCs were transduced with EV or STING before stimulation with 1,000 eggs per well. Cell lysates were used for western blot analysis using Abs against CD209a, STING, and GAPDH. (*D*) BMDCs from BL/6 and *STING*$^{-/-}$ mice were transduced with EV, shRNA against enhanced green fluorescent protein (EGFP) (shEGFP), or shRNA against CD209a (shCD209a) and then stimulated with 100 eggs for 24 h. IL-1β (*Left*) and IL-17 (*Right*) in culture supernatants were measured by ELISA. (*E*) 2 × 10^6 BL/6 and *STING*$^{-/-}$ BMDCs, (*F*) cGAS$^{-/-}$ BMDC and (*G*) IFNAR1$^{-/-}$ BMDC were plated in six-well plates and stimulated with 1,000 eggs for 24 h. *STING*$^{-/-}$ BMDCs were also pretreated with 2,000 units/mL rIFNβ before stimulation with 1,000 eggs per well. Bars represent the mean ± SD cytokine levels of three biological replicates from one representative experiment of three with similar results. *$P \leq 0.05$, **$P \leq 0.005$, ***$P \leq 0.0005$.

activates Janus kinases (JAK1/Tyk2) and signal transducers and activators of transcription (STAT1/2) leading to the dimerization, nuclear translocation, and binding to IRF9, thereby forming the ISG factor 3 (ISGF3) complex. This complex then binds to IFN-stimulated response elements (ISRE), leading to the transcription of a myriad ISGs (28). STAT1 has been reported to have dual functions, activating, or repressing transcription, depending on the context of promoters by recruiting coactivators or corepressors (35, 36). Previous studies showed that schistosome eggs are potent inducers of STAT1 phosphorylation in BL/6 DCs (19) but revealed no consequences to this activation. Our studies using STAT1 inhibitor fludarabine suggest that STAT1 is activated and required for egg-mediated IFNβ production in BL/6 BMDCs (*SI Appendix*, Fig. S4A). To investigate whether STAT1 activation by egg-mediated IFN-I was able to trigger the suppression of CD209a transcription, we used an EGFP reporter assay. By treating CD209a promoter-EGFP transduced BL/6 BMDCs with increasing concentrations of STAT1 inhibitor, we determined that STAT1 triggers the suppression of CD209a promoter activity (*SI Appendix*, Fig. S4B). While the exogenous IFNβ efficiently induced significant inhibition of CD209a promoter activity, STAT1 inhibition followed by the addition of IFNβ failed to do so (Fig. 5 *A*, *Left*), suggesting that STAT1 activation by IFN-I is necessary to inhibit CD209a transcription. Consistent with our pharmacological results, $STAT1^{-/-}$ BMDCs exhibited enhanced CD209a promoter activity (Fig. 5 *A*, *Right*). The addition of exogenous IFNβ failed to repress CD209a promoter activity in the absence of STAT1 while it efficiently inhibited the CD209a promoter activity in $STING^{-/-}$ cells, further demonstrating that STAT1 is required to suppress CD209a transcription (Fig. 5 *A*, *Right*). Pharmacological inhibition of STAT1 led to a significant increase in IL-1β (*SI Appendix*, Fig. S4 *C*, *Left*) and IL-17

(*SI Appendix*, Fig. S4 *C*, *Center*) secretion in BL/6 BMDCs but did not affect TNFα production in these cells (*SI Appendix*, Fig. S4 *C*, *Right*). In line with these data and similar to $STING^{-/-}$ BMDCs (Fig. 1 *F* and *L*, *Left*), IL-1β (Fig. 5 *B*, *Left*) and IL-17 (Fig. 5 *B*, *Right*) levels were enhanced in $STAT1^{-/-}$ cells. To understand whether STAT1-mediated suppression of CD209a can affect cytokine production, we silenced CD209a expression in BL/6 and $STAT1^{-/-}$ BMDCs (*SI Appendix*, Fig. S4D), which significantly reduced IL-1β (Fig. 5 *B*, *Left*) and IL-17 (Fig. 5 *B*, *Right*) expression in response to schistosome eggs. Overall, these data demonstrate that by directly suppressing CD209a expression, the STING–IFNβ–STAT1 axis limits proinflammatory and Th17 cytokine responses and downstream pathology.

Gsdmd Is Highly Expressed in CBA BMDCs and Suppresses Protective Egg-Mediated IFN-I by Reducing cGAS/STING Expression and Inducing Pyroptosis. We and others have previously shown that caspase-1 is required for egg-mediated IL-1β production (6, 37). Gsdmd has been recently discovered as a substrate for inflammatory caspases such as caspase-1 (38–40). Caspase-mediated cleavage of Gsdmd liberates the N-terminal fragment, which forms pores in the cell membrane, serving to facilitate the release of IL-1β and IL-18 upon inflammasome activation and also promote pyroptosis (41–44). Our previous gene array data suggested that Gsdmd mRNA levels are elevated in egg-stimulated and -unstimulated CBA BMDCs as compared to their BL/6 counterparts (7). As previously noted, pyroptosis is a feature of egg-induced IL-1β production (45, 46) and now we show that levels of uncleaved and cleaved (active N-terminal fragment) Gsdmd are increased in egg-stimulated CBA BMDCs (*SI Appendix*, Fig. S5A). To better understand how Gsdmd impacts egg-induced cGAS/STING-dependent
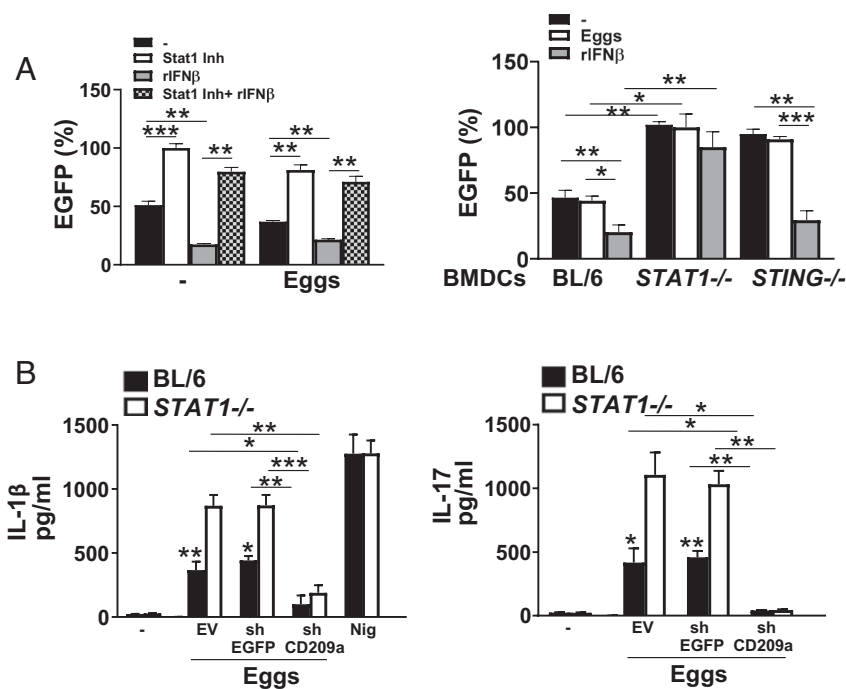

Fig. 5. IFN-I suppresses CD209a promoter activity via STAT1. (*A*) BMDCs from BL/6 mice were transduced with EV (not shown) or CD209a-promoter-EGFP and then pretreated with 5 μg of STAT1 inhibitor fludarabine phosphate for 1 h alone or before stimulating with 2,000 units/mL rIFNβ. Some cells were stimulated with just rIFNβ. The cells were then stimulated with 100 eggs for 24 h. EGFP levels were measured using a plate reader. Data presented as the percentage of EGFP, with EGFP levels in STAT1 inhibitor (Inh)-treated BMDCs being set at 100%. (*Left*). BMDCs from BL/6, $STAT1^{-/-}$, and $STING^{-/-}$ mice were transduced with EV (not shown) or CD209a-promoter-EGFP and then pretreated with 2,000 units/mL rIFNβ before stimulation with 100 eggs for 24 h (*Right*). Data presented as the percentage of EGFP, with EGFP levels in untreated $STAT1^{-/-}$ BMDCs being set at 100%. (*B*) BMDCs from BL/6 and $STAT1^{-/-}$ mice were transduced with EV or CD209a-promoter-EGFP before stimulation with 100 eggs for 24 h. IL-1β (*Left*) and IL-17 (*Right*) in supernatants were assessed by ELISA. For the purpose of measuring IFNβ and IL-1β, cultures proceeded for 24 h, and for IL-17, cultures also included CD4 T cells and proceeded for 72 h. Bars represent the mean ± SD cytokine levels of three biological replicates from one representative experiment of three with similar results. *$P \leq 0.05$, **$P \leq 0.005$, ***$P \leq 0.0005$, ns: not significant.

IFN-I production, we treated CBA BMDCs with the Gsdmd inhibitor dimethyl fumarate (47). The loss of Gsdmd markedly enhanced egg-dependent cGAS and STING expression (Fig. 6 *A*, *Left*), as well as IFNβ (Fig. 6 *A*, *Center*), while repressing IL-1β production (Fig. 6 *A*, *Right*). This suggests that Gsdmd exerts an inhibitory effect on IFN-I production by suppressing cGAS/STING expression. In support of this notion, retroviral overexpression of Gsdmd in BL/6 BMDCs reduced cGAS and STING expression (Fig. 6 *B*, *Left*), induced IFNβ (Fig. 6 *B*, *Center*), and suppressed IL-1β (Fig. 6 *B*, *Right*) production. To test whether Gsdmd expression or activity is required for this suppressive effect, we leveraged a Gsdmd mutant containing an isoleucine to asparagine mutation at position 105 (I105N) that abrogates the capacity of Gsdmd to oligomerize, form pores, and induce pyroptosis (41). In contrast to the effect of ectopic overexpression of Gsdmd, I105N Gsdmd-expressing cells displayed unchanged cGAS/STING (Fig. 6 *B*, *Left*) and IFNβ (Fig. 6 *B*, *Center*) expression with no enhancement of IL-1β (Fig. 6 *B*, *Right*) over controls. These findings suggest that the activity of Gsdmd, potentially in porulating cell membranes, is critical for suppressing the IFN-I pathway. We confirmed this using $Gsdmd^{-/-}$ BMDCs, which, in agreement with the Gsdmd inhibitor (Fig. 6*A*), enhanced cGAS and STING expression (Fig. 6 *C*, *Left*) and egg-induced IFNβ production (Fig. 6 *C*, *Center Left*), while reducing IL-1β (Fig. 6 *C*, *Center Right*) and IL-17 (Fig. 6 *C*, *Right*). Consistent with these findings, the enzymatic activity of cGAS was also enhanced in $Gsdmd^{-/-}$ BMDCs in response to eggs, as the intracellular levels of cGAMP in egg-stimulated $Gsdmd^{-/-}$ cells were significantly higher than

their WT counterparts (Fig. 6*D*). Additionally, STING is highly phosphorylated in egg-stimulated $Gsdmd^{-/-}$ BMDCs (*SI Appendix*, Fig. S5*B*). Given the critical impact of the I105N mutation, we surmised that Gsdmd suppresses cGAS/STING function by inducing egg-mediated pyroptosis. To directly test this, we compared cell survival in egg-stimulated CBA and BL/6 BMDCs as assessed by the vital probe calcein AM. As expected, in BL/6 BMDCs, there was significantly less cell death, which was largely dependent on Gsdmd since in $Gsdmd^{-/-}$ cells it was absent (Fig. 6*E*). More relevantly, the cell survival of $cGAS^{-/-}$ and $STING^{-/-}$ BMDCs was comparable to that of CBA BMDCs (Fig. 6*E*), suggesting that cGAS and STING negatively regulate Gsdmd-mediated pyroptosis.

Discussion

Our study elucidates the basis of disease heterogeneity in schistosome infection. We implicate the cGAS/STING intracellular DNA-sensing pathway in averting severe disease in murine schistosomiasis by regulating IL-1β and pathogenic Th17 responses. The absence of STING resulted in exacerbated egg-induced hepatic granulomatous inflammation, amidst an enhanced Th17/Th1, and diminished Th2 cytokine milieu. Similar shifts in cytokine production were also observed in an in vitro model, using egg-stimulated $STING^{-/-}$ BMDC- T cell cocultures. Consistent with several previous studies describing its antiinflammatory or homeostatic role (48–52), our results reveal a unique application of STING signaling as a key regulator of schistosome egg-induced immunopathology. We now show that cGAS/STING-dependent
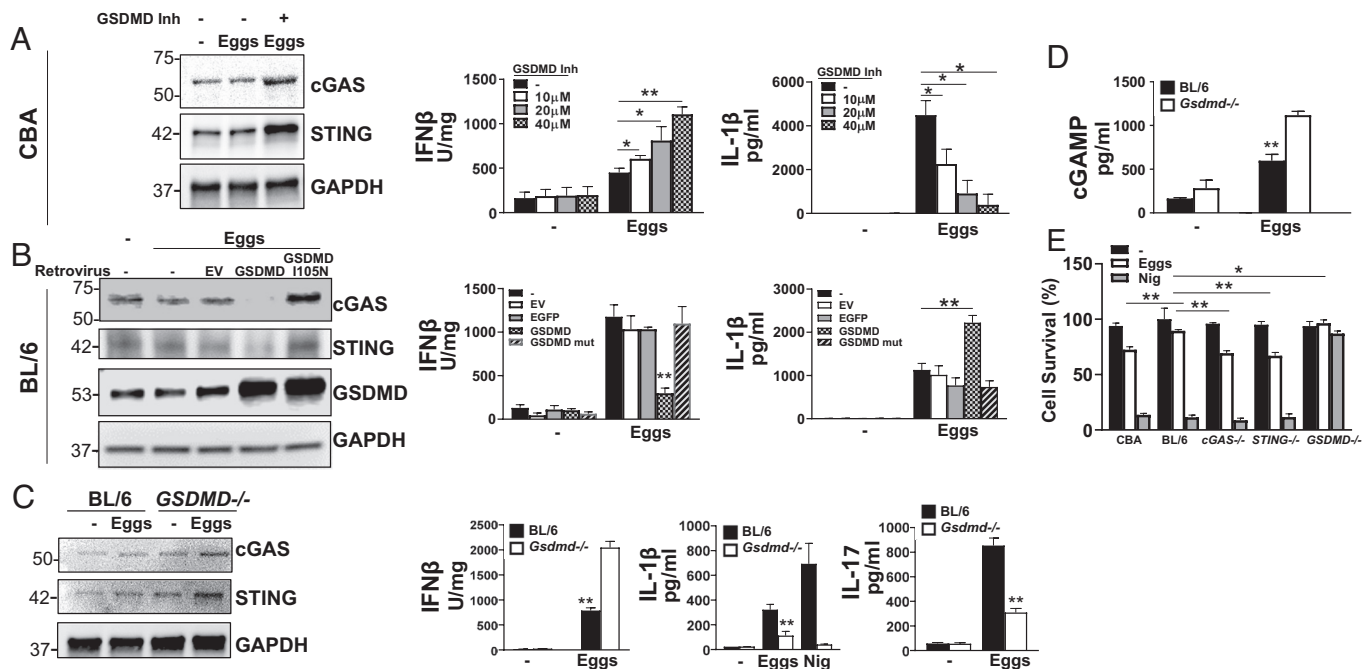

Fig. 6. Gsdmd promotes Th1 and Th17 cytokines while it suppresses protective IFN-I by inducing pyroptosis in response to schistosome eggs. (*A*) Immunoblot analysis of 2 × 10⁶ CBA BMDCs plated in six-well plates and pretreated with Gsdmd inhibitor dimethyl fumarate (25 μM) for 1 h before stimulating with 1,000 live eggs per well for 24 h. Cell lysates were used for western blot analysis using Abs against cGAS, STING, and GAPDH (*Left*). CBA BMDCs were treated with various concentrations of dimethyl fumarate for 1 h and then stimulated with 100 eggs. IFNβ (*Center*) and IL-1β (*Right*) in 24 h supernatants were assessed by ELISA. (*B*) BMDCs from BL/6 mice were transduced with EV, GSDMD, or GSDMD mutant (I105N) and then stimulated with 100 eggs for 24 h. Cell lysates were used for western blot analysis using Abs against cGAS, STING, GSDMD, and GAPDH (*Left*). IFNβ (*Center*) and IL-1β (*Right*) in 24 h supernatants were assessed by ELISA. (*C*) BMDCs from BL/6 and $GSDMD^{-/-}$ mice were stimulated with 100 eggs for 24 h. Cell lysates were used for western blot analysis using Abs against cGAS, STING, and GAPDH (*Left*). IFNβ (*Center Left*), IL-1β (*Center Right*), and IL-17 (*Right*) in supernatants were assessed by ELISA. For the purpose of measuring IFNβ and IL-1β cultures proceeded for 24 h, and for IL-17, cultures also included CD4 T cells and proceeded for 72 h. (*D*) 2 × 10⁶ BL/6 and $GSDMD^{-/-}$ BMDCs were plated in six-well plates and cultured with or without 1,000 eggs per well for 24 h. cGAMP was then measured in cell lysates using ELISA. (*E*) BMDCs from BL/6, $STING^{-/-}cGAS^{-/-}$, and $GSDMD^{-/-}$ mice were stimulated with 100 eggs or LPS plus nigericin (Nig) for 24 h. Cell survival was measured using calcein AM. Untreated BL/6 BMDCs were set to 100%. Bars represent the mean ± SD cytokine levels of three biological replicates from one representative experiment of three with similar results. *$P \leq 0.05$, **$P \leq 0.005$, ***$P \leq 0.0005$.

IFN-I-mediated STAT1 signaling down-regulates DC expression of CD209a, with consequent dampening of IL-1β, IL-23, and Th17 cell activation, as well as increased Th2 cytokines, resulting in the amelioration of immunopathology. A role of IFN-I in Th2 cell induction by DCs in response to schistosome eggs has been previously reported (18), although its broader impact on the in vivo infection and disease severity was not explored.

We demonstrate that Gsdmd, which is highly expressed in CBA BMDCs, restricts egg-mediated IFN-I responses via induction of pore formation and enhanced pyroptosis. These findings uncovered a unique interferon regulatory element in the context of a parasitic disease. A recent study shows that Gsdmd targets cGAS activation by disrupting ionic homeostasis (53), suggesting that Gsdmd-mediated inhibition of IFN-I pathway is exerted by various mechanisms depending on the stimulus/pathogen and/or cell type. Many studies have established the pathogenic role of inflammasomes in schistosome infection (37, 54–56). We now propose a model integrating the findings of this study with the previous ones in the context of downstream pathological impact: Eggs can activate both the cGAS/STING/IFNAR1/STAT1 and inflammasome pathways. In the low-pathology setting, cGAS/STING-dependent IFN-I is preferentially engaged by DNA released from eggs, presumably due to the high expression of these molecules in this genetic background. In the high-pathology setting, inflammasome and Gsdmd activation leads to predominantly pyroptotic and IL-1β-driven immune responses, and is accompanied by a further reduction in the expression of the immunoprotective cGAS/STING and IFN-I. These findings represent a significant conceptual advance in our understanding of the crosstalk between two major cytosolic immune surveillance pathways and its direct application in explaining schistosome egg-induced variability in immunopathology.

IFN-I-mediated immunosuppression can be employed by dissimilar mechanisms depending on the disease setting (57–60). Suppression of proinflammatory cytokines and Th17 responses in our system occurs at the level of *Cd209a* transcription. This inhibition requires STAT1 and thus this inhibitory effect can be a consequence of binding of STAT1 dimers or ISGF3 to the *Cd209a* promoter. STAT1-mediated activation of a transcriptional repressor might be an alternative mechanism by which STAT1 exerts its antiinflammatory function. Most importantly, CD209a promoter polymorphisms have been associated with responsiveness to IFN treatment (61) as well as increased susceptibility to a number of diseases (14, 61–63). The observed STING-dependent downregulation of CD209a was a specific phenomenon and not a global effect on all CLRs as Dectin-2 expression was not affected by the presence or absence of STING. Of note, IFN-I-mediated STAT1 activation has been shown to directly curb inflammation by inhibiting NLRP3 and IL-1β release (64). This could also be true in the context of schistosome infection, since NLRP3 inflammasome activation by schistosome eggs is well established (37, 65, 66). Although we present a previously unrecognized role of the cGAS/STING/IFNAR1/STAT1 axis in suppressing CD209a expression and attenuation of disease severity, we do not rule out the possible contribution of other pathway(s) by which IFN-I exerts its antiinflammatory function. A preponderance of evidence suggests that STING induces autophagy (67, 68) which in turn negatively regulates inflammasome activation by targeting individual inflammasome components as substrates for autophagic degradation (69–72). This represents another modality by which STING activation could prevent excessive inflammation in schistosome immunopathology.

We observed increased baseline CD209a expression in livers obtained from *STING*−/− mice and BMDCs, suggesting a role for constitutive (tonic) IFN signaling. Constitutive IFN-I has been shown to be dependent upon the STING pathway (33) and known to sustain steady-state levels of key players in the IFN signaling pathway, equipping the host cells to induce a rapid immune response at the time of schistosome infection (73, 74). We interpret these results as evidence that protective antiinflammatory mechanisms and predisposition to hyporeactivity exist in WT BL/6 but not *STING*−/− or CBA uninfected mice. Although CD209a levels were higher in both uninfected and infected *STING*−/− mice, Th17/Th1 cytokines have been detected in vivo and in vitro, respectively, in infected *STING*−/− mice and egg-stimulated *STING*−/− BMDCs. Thus, the heightened Th17/Th1 responses may result from interactions between schistosome eggs and a host deficient in STING. Indeed, a homeostatic role for STING has been previously proposed (30, 50, 75, 76). These results indicate that CD209a must be transcriptionally modulated by STING-dependent tonic IFN-I levels, making it a unique target downstream of STING/IFN-I signaling.

Although it has previously been suggested that IFN-I is produced by DCs stimulated with egg Ags, a possible role for cytosolic DNA sensing has not been investigated. Webb et al. reported that the IFNα3 response to soluble egg Ag (SEA) by in vitro-generated Flt3-L BMDCs is dependent on the adaptor molecule TRIF (18) and is negatively regulated by MyD88 but they did not address the impact of TRIF or MyD88 deficiency on Th polarization nor whether these molecules have a role in the immunopathology. On the one hand, TRIF deficiency in conventional DCs (cDCs) did not alter IFNβ production in response to eggs. On the other hand, IFN-I production by plasmocytoid DCs (pDCs) was shown to be MyD88 dependent (28). Additionally, various IFN-I subtypes have distinct biological activities (77). Therefore, different DC subsets, Ags, and IFN-I subtypes might explain the observed disparities.

An unresolved question in our current study and a major gap in the field is by what mechanisms DNA gains access to the cytosol of DCs in vivo. Candidate molecules responsible for DNA transfer are the peptide LL37 (78), CLEC9A receptor (79), and high-mobility group box 1 (HMGB1) (80), which act by various mechanisms to take up DNA from extracellular sources. The specific contribution of these factors remains to be defined. We do not rule out the contribution of host cell death as a potential source of DNA, however at the doses used in our studies, schistosome eggs did not significantly impact cell viability (6).

Activation of the STING pathway with consequent IFN-I production is critical for host defense against pathogens (81); however, its excessive activation may lead to the development of autoimmune diseases such as systemic lupus erythematosus (62) and Aicardi–Goutieres syndrome (82). Our results suggest that activation of STING with *S. mansoni* DNA leads to the production of IFN-I that suppresses proinflammatory cytokine production. Based on these results, it would be highly likely that pharmacological activation of STING with STING agonists or cyclic dinucleotides (CDN) could ameliorate egg-induced immunopathology. Such an approach has proven to be successful in the attenuation of antigen-induced arthritis (AIA) and Experimental autoimmune encephalomyelitis (EAE) (48, 83). Furthermore, our results indicating that stimulation with rIFN-I leads to a decrease in CD209a expression and proinflammatory cytokine production suggest the possible beneficial effect of IFN-based therapy in vivo.

Materials and Methods

Mice, Parasites, and Infection. Five- to six-week-old female CBA/J, C57BL/6, *TRIF*−/−, *IFNAR1*−/−, *STAT1*−/−, and *GSDMD*−/− mice were purchased from The Jackson Laboratory and Swiss Webster mice from Taconic Biosciences.

cGAS^{−/−} mice were from Katherine Fitzgerald and *STING*^{−/−} mice were from Alexander Poltorak. Breeding colonies were established for *STING*^{−/−}, *IFNAR1*^{−/−}, and *cGAS*^{−/−} mice. All mice were maintained at the Tufts University School of Medicine Animal Facility in accordance with the Association for Assessment and Accreditation of Laboratory Animal Care guidelines. The mice were infected by i.p. injection with 85 cercariae of *S. mansoni* (Puerto Rico strain) shed from infected *Biomphalaria glabrata* snails. The snails were provided by the NIAID Schistosomiasis Resource Center of the Biomedical Research Institute (Rockville, MD) through NIH-NIAID Contract HHSN272201000005I for distribution through BEI Resources. Live schistosome eggs were isolated from livers of infected Swiss Webster mice under sterile conditions by a series of blending and straining techniques, as previously described (84).

Reagents. RPMI 1640 medium was from Lonza, FBS was from Atlanta Biologicals, glutamine and penicillin-streptomycin were from Gibco, and recombinant murine GM-CSF was from PeproTech. Murine recombinant (r) IFNβ was from Pbl Assay Science. Dimethyl fumarate, Poly (dAdT), Red Blood Cell Lysing Buffer, fludarabine phosphate, and 2-mercaptoethanol were from Sigma. LPS was from Invivogen. Calcein AM was from Invitrogen. GeneJuice was from Novagen. *S.mansoni* genomic DNA was from the Schistosomiasis Resource Center (NIH).

Cells, Cell Cultures, and Cell Stimulations. Restimulation of bulk lymphoid cells. Spleen cells and MLNs from 7 wk-infected BL/6 and *STING*^{−/−} mice were prepared as previously described (85). 2 × 10⁵ cells were plated and stimulated with 100 live eggs for 72 h.

DC cultures. BMDCs were generated as described previously (6). 2 × 10⁵ BMDCs were plated and stimulated with 100 live eggs. Some cells were stimulated with LPS (100 ng/mL) for 24 h followed by nigericin (10 μM) for 1 h.

DC-T cell cocultures. CD4⁺ T cells were prepared from normal BL/6 spleens using a CD4⁺ T Cell Isolation Kit II for mouse (Miltenyi Biotec, Cambridge, MA) in accordance with the manufacturer's instructions. Purified CD4⁺ T cells (2 × 10⁵) were cultured with 10⁵ syngeneic BMDCs and stimulated with 100 live eggs plus 8 × 10⁴ anti-CD3/CD28-coated beads (Gibco Dynal Dynabeads) for 72 h.

ELISA and Quantitative RT-PCR. Cytokine protein measurements were performed in culture supernatants and tissue homogenates for IL-1β, IL-23, IL-17A, IFNγ, TNFα, IL-4, IL-5, IL-13, and IFNβ using ELISA kits from R&D Systems in accordance with the manufacturer's instructions. cGAMP was measured in BMDCs lysed with RIPA buffer using 2′3′-cGAMP ELISA kit (Arbor Assays) in accordance with the manufacturer's instructions. Spleens and livers from 7-wk-infected mice were homogenized, and total protein concentrations were determined using a BCA protein assay kit (Thermo Scientific). RNA was obtained from cultured cells and spleen and liver homogenates using TRIzol Reagent (Ambion) or PureLink RNA kit (Ambion) and measured for CD209a mRNA levels. cDNA was synthesized with a HighCapacity cDNA RT Kit (Applied Biosystems) and TaqMan probes for *cd209a* and *Gapdh* in combination with TaqMan Gene Expression Master Mix (all from Applied Biosystems).

Liver Pathology and Immunofluorescence Studies. Liver samples obtained from the infected mice were fixed in 10% buffered formalin, processed and sectioned by routine histopathologic technique, stained with H&E, and examined by light microscopy. Blinded morphometric analysis was performed using Image-Pro Plus software as described previously described (85) to measure the size of individual hepatic granulomas with visible central eggs.

Retro/Lentiviral Production and Retro/Lentiviral Transduction. Full-length murine STING was cloned into the pRetro-Zeocin (pRZ) vector and tagged with HA and citrine. Retroviral vectors were packaged using the retroviral packaging vectors and vesicular stomatitis virus-glycoprotein (VSV-G) pseudotyping vector. Viral particles were produced in HEK293T cells using GeneJuice Transfection Reagent (Novagen). Retroviruses expressing STING or the EV were used to infect BMDCs, as previously described (86). Overexpression of STING was verified by western blot analysis.

HEK293T cells were transfected with pMSCV-puro encoding 2xFLAG-HA-Gsdmd, or MSCV-puro encoding 2xFLAG-HA-I105N Gsdmd mutant and retroviral packaging plasmids and VSV-G pseudotyping vector. Viral particles were produced as explained above. Retroviruses expressing EV, Gsdmd, or mutant Gsdmd were used to infect BMDCs, as previously described (86). Overexpression of Gsdmd was verified by western blot and qPCR analysis.

CD209a-promoter was cloned into the pEZX-LvPF02 vector with eGFP reporter gene (GeneCopoeia). Lentiviral vectors were packaged using the packaging vector psPAX2 and the VSV-G pseudotyping vector pMD2 as previously described (6). Viral particles were produced in HEK293T cells using GeneJuice Transfection Reagent (Novagen). Lentiviruses expressing EV or CD209a-promoter were used to infect BMDCs, as previously described (7).

RNA Interference. BMDCs were transduced with lentiviruses containing lentiviral TRC shRNA expression plasmids targeting CD209a (Dharmacon). TRC EGFP shRNA was designed against the enhanced GFP reporter (Dharmacon). The production of viral particles and transduction of BMDCs were conducted as described previously (6).

Western Blotting. BMDCs were washed, lysed, and prepared with Laemmli Buffer (Boston BioProducts). Samples were run on an SDS-PAGE gel and transferred to a nitrocellulose membrane (BioRad), which was blocked in 5% BSA. Protein expression was detected with Abs specific for MyD88 (AF3109, R&D Systems), MAVS (4983, Cell Signaling), STING (24683, Novus Biologicals), CD209a (95634, Abcam), cGAS (31659, Cell Signaling), gasdermin D (209845, Abcam), Dectin-2 (BAF1525, R&D Systems), phospho-STING (Ser 365) (72971, Cell Signaling), and GAPDH (2118; Cell Signaling).

Statistics. Student's *t* test was used for statistical analysis of differences between groups. *P* values ≤0.05 were considered significant.

Study Approval. All animal experiments in this study were approved by the Institutional Animal Care and Use Committee at Tufts and Pennsylvania State University.

Author affiliations: ^aDepartment of Immunology, Tufts University School of Medicine, Boston, MA 02111; and ^bDepartment of Veterinary and Biomedical Sciences, Center for Molecular Immunology and Infectious Disease, The Pennsylvania State University, University Park, PA 16802

1. D. P. McManus *et al.*, Schistosomiasis. *Nat. Rev. Dis. Primers* **4**, 13 (2018).
2. E. J. Pearce, A. S. MacDonald, The immunobiology of schistosomiasis. *Nat. Rev. Immunol.* **2**, 499–511 (2002).
3. A. W. Cheever *et al.*, Variation of hepatic fibrosis and granuloma size among mouse strains infected with Schistosoma mansoni. *Am. J. Trop. Med. Hyg.* **37**, 85–97 (1987).
4. P. M. Smith *et al.*, Genetic control of severe egg-induced immunopathology and IL-17 production in murine schistosomiasis. *J. Immunol.* **183**, 3317–3323 (2009).
5. H. J. Hernandez, W. C. Trzyna, J. S. Cordingley, P. H. Brodeur, M. J. Stadecker, Differential antigen recognition by T cell populations from strains of mice developing polar forms of granulomatous inflammation in response to eggs of Schistosoma mansoni. *Eur. J. Immunol.* **27**, 666–670 (1997).
6. P. Kalantari *et al.*, CD209a synergizes with Dectin-2 and Mincle to drive severe Th17 cell-mediated schistosome egg-induced immunopathology. *Cell Rep.* **22**, 1288–1300 (2018).

7. H. E. Ponichtera *et al.*, CD209a expression on dendritic cells is critical for the development of pathogenic Th17 cell responses in murine schistosomiasis. *J. Immunol.* **192**, 4655–4665 (2014).
8. P. Kalantari, S. C. Bunnell, M. J. Stadecker, The C-type lectin receptor-driven, Th17 cell-mediated severe pathology in schistosomiasis: Not all immune responses to helminth parasites are Th2 dominated. *Front. Immunol.* **10**, 26 (2019).
9. L. R. Brunet, F. D. Finkelman, A. W. Cheever, M. A. Kopf, E. J. Pearce, IL-4 protects against TNF-alpha-mediated cachexia and death during acute schistosomiasis. *J. Immunol.* **159**, 777–785 (1997).
10. D. R. Herbert *et al.*, Alternative macrophage activation is essential for survival during schistosomiasis and downmodulates T helper 1 responses and immunopathology. *Immunity* **20**, 623–635 (2004).
11. W. C. Gause, J. F. Urban Jr., M. J. Stadecker, The immune response to parasitic helminths: Insights from murine models. *Trends Immunol.* **24**, 269–277 (2003).

12. E. J. Pearce, P. Caspar, J. M. Grzych, F. A. Lewis, A. Sher, Downregulation of Th1 cytokine production accompanies induction of Th2 responses by a parasitic helminth, Schistosoma mansoni. *J. Exp. Med.* **173**, 159–166 (1991).

13. H. E. Ponichtera, M. J. Stadecker, Dendritic cell expression of the C-type lectin receptor CD209a: A novel innate parasite-sensing mechanism inducing Th17 cells that drive severe immunopathology in murine schistosome infection. *Exp. Parasitol.* **158**, 42–47 (2015).

14. T. B. Geijtenbeek *et al.*, DC-SIGN, a dendritic cell-specific HIV-1-binding protein that enhances trans-infection of T cells. *Cell* **100**, 587–597 (2000).

15. J. den Dunnen, S. I. Gringhuis, T. B. Geijtenbeek, Innate signaling by the C-type lectin DC-SIGN dictates immune responses. *Cancer Immunol. Immunother* **58**, 1149–1157 (2009).

16. I. van Die *et al.*, The dendritic cell-specific C-type lectin DC-SIGN is a receptor for Schistosoma mansoni egg antigens and recognizes the glycan antigen Lewis x. *Glycobiology* **13**, 471–478 (2003).

17. A. Marzi *et al.*, The signal peptide of the ebolavirus glycoprotein influences interaction with the cellular lectins DC-SIGN and DC-SIGNR. *J. Virol.* **80**, 6305–6317 (2006).

18. L. M. Webb *et al.*, Type I interferon is required for T helper (Th) 2 induction by dendritic cells. *EMBO J.* **36**, 2404–2418 (2017).

19. F. Trottein *et al.*, A type I IFN-dependent pathway induced by Schistosoma mansoni eggs in mouse myeloid dendritic cells generates an inflammatory signature. *J. Immunol.* **172**, 3011–3017 (2004).

20. H. Ishikawa, G. N. Barber, STING is an endoplasmic reticulum adaptor that facilitates innate immune signalling. *Nature* **455**, 674–678 (2008).

21. D. L. Burdette, R. E. Vance, STING and the innate immune response to nucleic acids in the cytosol. *Nat. Immunol.* **14**, 19–26 (2013).

22. Q. Chen, L. Sun, Z. J. Chen, Regulation and function of the cGAS-STING pathway of cytosolic DNA sensing. *Nat. Immunol.* **17**, 1142–1149 (2016).

23. C. Gallego-Marin *et al.*, Cyclic GMP-AMP synthase is the cytosolic sensor of Plasmodium falciparum genomic DNA and activates type I IFN in malaria. *J. Immunol.* **200**, 768–774 (2018).

24. D. Gao *et al.*, Cyclic GMP-AMP synthase is an innate immune sensor of HIV and other retroviruses. *Science* **341**, 903–906 (2013).

25. A. C. Collins *et al.*, Cyclic GMP-AMP synthase is an innate immune DNA sensor for Mycobacterium tuberculosis. *Cell Host Microbe* **17**, 820–828 (2015).

26. S. R. Paludan, A. G. Bowie, Immune sensing of DNA. *Immunity* **38**, 870–880 (2013).

27. O. Takeuchi, S. Akira, Pattern recognition receptors and inflammation. *Cell* **140**, 805–820 (2010).

28. F. McNab, K. Mayer-Barber, A. Sher, A. Wack, A. O'Garra, Type I interferons in infectious disease. *Nat. Rev. Immunol.* **15**, 87–103 (2015).

29. G. D. Kalliolias, L. B. Ivashkiv, Overview of the biology of type I interferons. *Arthritis Res. Ther.* **12** (suppl. 1), S1 (2010).

30. S. Sharma, K. A. Fitzgerald, M. P. Cancro, A. Marshak-Rothstein, Nucleic acid-sensing receptors: Rheostats of autoimmunity and autoinflammation. *J. Immunol.* **195**, 3507–3512 (2015).

31. K. Honda *et al.*, Spatiotemporal regulation of MyD88-IRF-7 signalling for robust type-I interferon induction. *Nature* **434**, 1035–1040 (2005).

32. M. O. Ullah, M. J. Sweet, A. Mansell, S. Kellie, B. Kobe, TRIF-dependent TLR signaling, its functions in host defense and inflammation, and its potential as a therapeutic target. *J. Leukoc. Biol.* **100**, 27–45 (2016).

33. J. Sarhan *et al.*, Constitutive interferon signaling maintains critical threshold of MLKL expression to license necroptosis. *Cell Death Differ.* **26**, 332–347 (2019).

34. M. Relloso *et al.*, DC-SIGN (CD209) expression is IL-4 dependent and is negatively regulated by IFN, TGF-beta, and anti-inflammatory agents. *J. Immunol.* **168**, 2634–2643 (2002).

35. J. Torchia, C. Glass, M. G. Rosenfeld, Co-activators and co-repressors in the integration of transcriptional responses. *Curr. Opin. Cell Biol.* **10**, 373–383 (1998).

36. C. V. Ramana, M. Chatterjee-Kishore, H. Nguyen, G. R. Stark, Complex roles of Stat1 in regulating gene expression. *Oncogene* **19**, 2619–2627 (2000).

37. M. Ritter *et al.*, Schistosoma mansoni triggers Dectin-2, which activates the Nlrp3 inflammasome and alters adaptive immune responses. *Proc. Natl. Acad. Sci. U.S.A.* **107**, 20459–20464 (2010).

38. W. T. He *et al.*, Gasdermin D is an executor of pyroptosis and required for interleukin-1beta secretion. *Cell Res.* **25**, 1285–1298 (2015).

39. N. Kayagaki *et al.*, Caspase-11 cleaves gasdermin D for non-canonical inflammasome signalling. *Nature* **526**, 666–671 (2015).

40. J. Shi *et al.*, Cleavage of GSDMD by inflammatory caspases determines pyroptotic cell death. *Nature* **526**, 660–665 (2015).

41. R. A. Aglietti *et al.*, GsdmD p30 elicited by caspase-11 during pyroptosis forms pores in membranes. *Proc. Natl. Acad. Sci. U.S.A.* **113**, 7858–7863 (2016).

42. J. Ding *et al.*, Pore-forming activity and structural autoinhibition of the gasdermin family. *Nature* **535**, 111–116 (2016).

43. X. Liu *et al.*, Inflammasome-activated gasdermin D causes pyroptosis by forming membrane pores. *Nature* **535**, 153–158 (2016).

44. J. Lieberman, H. Wu, J. C. Kagan, Gasdermin D activity in inflammation and host defense. *Sci. Immunol.* **4**, eaav1447 (2019).

45. D. L. Kong *et al.*, Soluble egg antigen of Schistosoma japonicum induces pyroptosis in hepatic stellate cells by modulating ROS production. *Parasit. Vectors* **12**, 475 (2019).

46. X. Liu *et al.*, Taurine alleviates schistosoma-induced liver injury by inhibiting the TXNIP/NLRP3 inflammasome signal pathway and pyroptosis. *Infect. Immun.* **87**, e00732-19 (2019).

47. F. Humphries *et al.*, Succination inactivates gasdermin D and blocks pyroptosis. *Science* **369**, 1633–1637 (2020).

48. H. Lemos *et al.*, Activation of the STING adaptor attenuates experimental autoimmune encephalitis. *J. Immunol.* **192**, 5571–5578 (2014).

49. V. Mathur *et al.*, Activation of the STING-dependent type I interferon response reduces microglial reactivity and neuroinflammation. *Neuron* **96**, 1290–1302.e6 (2017).

50. S. Sharma *et al.*, Suppression of systemic autoimmunity by the innate immune adaptor STING. *Proc. Natl. Acad. Sci. U.S.A.* **112**, E710–E717 (2015).

51. Q. Zhao, M. Manohar, Y. Wei, S. J. Pandol, A. Habtezion, STING signalling protects against chronic pancreatitis by modulating Th17 response. *Gut* **68**, 1827–1837 (2019).

52. D. S. Lima-Junior *et al.*, Endogenous retroviruses promote homeostatic and inflammatory responses to the microbiota. *Cell* **184**, 3794–3811.e19 (2021).

53. I. Banerjee *et al.*, Gasdermin D restrains type I interferon response to cytosolic DNA by disrupting ionic homeostasis. *Immunity* **49**, 413–426.e5 (2018).

54. N. Meng *et al.*, Activation of NLRP3 inflammasomes in mouse hepatic stellate cells during Schistosoma J. infection. *Oncotarget* **7**, 39316–39331 (2016).

55. Y. Q. Lu, S. Zhong, N. Meng, Y. P. Fan, W. X. Tang, NLRP3 inflammasome activation results in liver inflammation and fibrosis in mice infected with Schistosoma japonicum in a Syk-dependent manner. *Sci. Rep.* **7**, 8120 (2017).

56. B. J. Ferguson *et al.*, The Schistosoma mansoni T2 ribonuclease omega-1 modulates inflammasome-dependent IL-1beta secretion in macrophages. *Int. J. Parasitol.* **45**, 809–813 (2015).

57. L. M. Snell, D. G. Brooks, New insights into type I interferon and the immunopathogenesis of persistent viral infections. *Curr. Opin. Immunol.* **34**, 91–98 (2015).

58. S. J. Bergman, M. C. Ferguson, C. Santanello, Interferons as therapeutic agents for infectious diseases. *Infect. Dis. Clin. North Am.* **25**, 819–834 (2011).

59. IFNB Multiple Sclerosis Study Group, Interferon beta-1b is effective in relapsing-remitting multiple sclerosis. I. Clinical results of a multicenter, randomized, double-blind, placebo-controlled trial. 1993 [classical article]. *Neurology* **57** (12 suppl. 5), S3–S9 (2001).

60. L. B. Ivashkiv, PTPN22 in autoimmunity: Different cell and different way. *Immunity* **39**, 91–93 (2013).

61. L. Zupin *et al.*, CD209 promoter polymorphisms associate with HCV infection and pegylated-interferon plus ribavirin treatment response. *Mol. Immunol.* **76**, 49–54 (2016).

62. L. B. Barreiro *et al.*, Promoter variation in the DC-SIGN-encoding gene CD209 is associated with tuberculosis. *PLoS Med.* **3**, e20 (2006).

63. R. C. da Silva *et al.*, Association of CD209 and CD209L polymorphisms with tuberculosis infection in a Northeastern Brazilian population. *Mol. Biol. Rep.* **41**, 5449–5457 (2014).

64. G. Guarda *et al.*, Type I interferon inhibits interleukin-1 production and inflammasome activation. *Immunity* **34**, 213–223 (2011).

65. T. T. W. Chen *et al.*, Activation of the NLRP3 and AIM2 inflammasomes in a mouse model of Schistosoma mansoni infection. *J. Helminthol.* **94**, e72 (2019).

66. W. J. Zhang, Z. M. Fang, W. Q. Liu, NLRP3 inflammasome activation from Kupffer cells is involved in liver fibrosis of Schistosoma japonicum-infected mice via NF-kappaB. *Parasit. Vectors* **12**, 29 (2019).

67. X. Gui *et al.*, Autophagy induction via STING trafficking is a primordial function of the cGAS pathway. *Nature* **567**, 262–266 (2019).

68. D. Liu *et al.*, STING directly activates autophagy to tune the innate immune response. *Cell Death Differ.* **26**, 1735–1749 (2019).

69. J. Harris *et al.*, Autophagy and inflammasomes. *Mol. Immunol.* **86**, 10–15 (2017).

70. J. Harris *et al.*, Autophagy controls IL-1beta secretion by targeting pro-IL-1beta for degradation. *J. Biol. Chem.* **286**, 9587–9597 (2011).

71. T. Saitoh *et al.*, Loss of the autophagy protein Atg16L1 enhances endotoxin-induced IL-1beta production. *Nature* **456**, 264–268 (2008).

72. C. S. Shi *et al.*, Activation of autophagy by inflammatory signals limits IL-1beta production by targeting ubiquitinated inflammasomes for destruction. *Nat. Immunol.* **13**, 255–263 (2012).

73. B. C. Liu, J. Sarhan, A. Poltorak, Host-intrinsic interferon status in infection and immunity. *Trends Mol. Med.* **24**, 658–668 (2018).

74. S. Mostafavi *et al.*, Parsing the interferon transcriptional network and its disease associations. *Cell* **164**, 564–578 (2016).

75. J. Li, S. F. Bakhoum, Expanding the role of STING in cellular homeostasis and transformation. *Trends Cancer* **5**, 195–197 (2019).

76. M. C. C. Canesso *et al.*, The cytosolic sensor STING is required for intestinal homeostasis and control of inflammation. *Mucosal. Immunol.* **11**, 820–834 (2018).

77. C. T. Ng, J. L. Mendoza, K. C. Garcia, M. B. Oldstone, Alpha and beta type 1 interferon signaling: Passage for diverse biologic outcomes. *Cell* **164**, 349–352 (2016).

78. R. Lande *et al.*, Plasmacytoid dendritic cells sense self-DNA coupled with antimicrobial peptide. *Nature* **449**, 564–569 (2007).

79. D. Sancho *et al.*, Identification of a dendritic cell receptor that couples sensing of necrosis to immunity. *Nature* **458**, 899–903 (2009).

80. H. Yanai *et al.*, HMGB proteins function as universal sentinels for nucleic-acid-mediated innate immune responses. *Nature* **462**, 99–103 (2009).

81. J. W. Schoggins *et al.*, Pan-viral specificity of IFN-induced genes reveals new roles for cGAS in innate immunity. *Nature* **505**, 691–695 (2014).

82. Y. J. Crow *et al.*, Mutations in the gene encoding the 3'-5' DNA exonuclease TREX1 cause Aicardi-Goutieres syndrome at the AGS1 locus. *Nat. Genet.* **38**, 917–920 (2006).

83. L. Huang *et al.*, Engineering DNA nanoparticles as immunomodulatory reagents that activate regulatory T cells. *J. Immunol.* **188**, 4913–4920 (2012).

84. M. G. Shainheit *et al.*, Dendritic cell IL-23 and IL-1 production in response to schistosome eggs induces Th17 cells in a mouse strain prone to severe immunopathology. *J. Immunol.* **181**, 8559–8567 (2008).

85. L. I. Rutitzky *et al.*, IL-23 is required for the development of severe egg-induced immunopathology in schistosomiasis and for lesional expression of IL-17. *J. Immunol.* **180**, 2486–2495 (2008).

86. P. Kalantari, O. F. Harandi, P. A. Hankey, A. J. Henderson, HIV-1 tat mediates degradation of RON receptor tyrosine kinase, a regulator of inflammation. *J. Immunol.* **181**, 1548–1555 (2008).